Materials Letters 379 (2025) 137665

Contents lists available at ScienceDirect

Materials Letters

journal homepage: www.elsevier.com/locate/matlet

SiC-induced modification of $MnCo_2O_4$ nanoneedles fabricated on Ni foam for binder-free electrodes in high-performance asymmetrical supercapacitors

Dajun Wu [a,*,1], Panyi Wu [a,1], Zhengpeng Xia [a], Xuekun Hong [a], Bin Qian [a], Paul K. Chu [b]

[a] Jiangsu Laboratory of Advanced Functional Materials, School of Electronic and Information Engineering, Changshu Institute of Technology, Changshu 215500, China
[b] Department of Physics, Department of Materials Science and Engineering, and Department of Biomedical Engineering, City University of Hong Kong, Tat Chee Avenue, Kowloon, Hong Kong, China

ARTICLE INFO

Keywords:
Supercapacitors
Quasi-Solid-State
SiC nanoparticles
$MnCo_2O_4$ nanoneedles

ABSTRACT

Supercapacitors with large energy densities are required for commercial applications. Herein, the urchin-like and hexagonal $MnCo_2O_4$/SiC composite is prepared *in situ* on Ni foam. The urchin-like $MnCo_2O_4$/SiC consists of nanoneedle clusters with a length of about 10 μm and a diameter of 20 nm. The $MnCo_2O_4$/SiC||AC asymmetrical supercapacitor (ASCs) shows an energy density of 90.3 Wh/kg (1.73F cm^{-2}) at a power density of 1.25 kW/kg together with 92.1 % retention of the specific capacitance after 10,000 cycles. The results reveal excellent properties and large commercial potential.

1. Introduction

Owing to advantages such as large power density, environmental friendliness, and safety, supercapacitors (SCs) have attracted much attention as energy storage devices. Manganese cobalt oxide (MCO) composites with a spinel structure, such as $MnCo_2O_4$ nanoneedles [1], $MnCo_2O_4$ nanosheets [2], $MnCo_2O_4$ microsphere [3], $MnCo_2O_4$ quasi-cubes [4], $MnCo_2O_4$ nanoflakes [5], and $MnCo_2O_4$ hollow nanospheres [6], are promising electroactive materials for SCs due to the good conductivity and multiple valence states compared to single metal oxides. Heteroatom doping has been used to modify the morphology and structure [7] to improve the energy-storage properties of $MnCo_2O_4$-based materials as supercapacitor electrodes, for instance, Fe/Ni/Zn-doped $MnCo_2O_4$ [8], Ag-$MnCo_2O_4$ [9], MnO_2/$MnCo_2O_4$ [10], and $MnCo_2O_4$@$CuCo_2O_4$ [11]. For example, Yu et al. have fabricated $MnCo_2O_4$/$Co_3V_2O_8$ with a specific capacitance of 1,460F g^{-1} at 1 A g^{-1} [12]. Mi and co-workers have synthesized $MnCo_2O_4$ @$Co(OH)_2$ with a maximum energy density of 55.42 Wh kg^{-1} and power density of 800.0 W kg^{-1} [13]. Li et al. have produced core–shell $MnCo_2O_4$/@NiCo-LDH/NF by hydrothermal preparation with electrochemical deposition, which shows a specific capacitance of 4555.0F g^{-1} at 1 A g^{-1} and capacitance retention of 78.7 % after 5,000 cycles [14]. Nevertheless, despite recent advances, $MnCo_2O_4$-based nanocomposites still have relatively low energy densities and inadequate cycling stability, and improvements must be made for commercial adoption.

Carbon spheres, activated carbon and silicon carbide have large surface areas for high energy densities [15]. Chang et al. have fabricated SiC Nws/YSZ/SiC NWs for supercapacitors with a maximum areal power density of 100 μW cm^{-2} [16], and the nano-cauliflower-like SiC nanostructure has a specific capacitance of 188F g-1 at 5 mV/s and energy density of 31.4 Wh kg^{-1} [17]. The supercapacitor electrode comprising microporous and mesoporous SiC/Fe_3O_4 composites exhibit a specific capacitance of 423.2F g^{-1} at 5 mV s^{-1} and high capacitance retention over a wide range of scanning rates (81.8 % at 500 mV s^{-1}) [18]. However, to the best of our knowledge, the novel morphology of SiC and Mn-based bimetal composite have seldom been investigated and its application to asymmetrical supercapacitors has not been demonstrated.

Herein, the urchin-like and hexagonal $MnCo_2O_4$/SiC composite is prepared on Ni foam *in situ* by magnetron sputtering and hydrothermal processing. The supercapacitor assembled with $MnCo_2O_4$/SiC||AC has excellent stability and energy density, boding well for the development of high-performance supercapacitors.

2. Experimental details

After the Ni-foam substrate was treated with oxygen plasma, SiC

* Corresponding author.
E-mail addresses: wdjyss2004@126.com (D. Wu), paul.chu@cityu.edu.hk (P. Wu), xkhong@cslg.edu.cn (X. Hong).
[1] The two co-first authors contributed equally to the work.

https://doi.org/10.1016/j.matlet.2024.137665
Received 30 August 2024; Received in revised form 30 October 2024; Accepted 3 November 2024
Available online 5 November 2024

coatings were fabricated by magnetron sputtering using Ar as the sputtering gas and high-purity SiC as the sputtering target. The DC power, substrate temperature, Ar gas flow, pressure, and deposition time were 80 W, 600 K, 45 sccm, 8 Pa, and 20 min, respectively. $MnCo_2O_4$ was deposited on the SiC/Ni foam by a hydrothermal technique. As shown in Figs. 1, 1 mmol $Mn(NO)_3{\cdot}6H_2O$, 2 mmol $Co(NO)_3{\cdot}6H_2O$, 5 mmol urea, and 6 mmol NH_4F were dissolved in 60 ml of deionized water and stirred for about 30 min. The solution was transferred to a 100 ml Teflon-lined stainless-steel autoclave in which a piece of SiC/Ni foam was placed in the solution. The autoclave was heated to 120 ℃ for 8 h, the product was rinsed with deionized water and ethanol for 5 min successively. The $MnCo_2O_4$/SiC/Ni foam was dried in vacuum at 60 ℃ overnight.

The morphology and crystallographic structure were examined by field-emission scanning electron microscopy (FE-SEM, Hitachi S-4800, and Japan) and high-resolution transmission electron microscopy (HR-TEM; Philips Tecanai G2 F30). The crystal structure was determined by X-ray diffraction (XRD, Rigaku, RINT2000, Japan). The supercapacitor was assembled with the $MnCo_2O_4$/SiC/Ni foam and AC/Ni foam electrodes to form a 2032-type button cell. The LAND CT2001A system was used to conduct galvanostatic charging-discharging (GCD), and the CHI760E (Chenhua, Shanghai) electrochemical workstation was employed for cyclic voltammetry (CV) and electrochemical impedance spectroscopy (EIS).

3. Results and discussion

Fig. 1 shows the schematic illustration of the synthesis of $MnCo_2O_4$/SiC composites on Ni foam. A two-step process, including *in situ* DC magnetron sputtering and hydrothermal processing, is carried out to deposit high-purity SiC films and $MnCo_2O_4$ on the Ni foam substrate. The SEM images of $MnCo_2O_4$/SiC are depicted in Fig. 2a-b. The urchin-like and hexagonal $MnCo_2O_4$/SiC composite composed of nanoneedle clusters with a length of 10 μm and diameter of 20 nm is distributed uniformly on the Ni foam. The hexagonal structure with a diameter of 4 μm also increases the surface area (Fig. 2c). As shown in Fig. 2e-i, the lattice fringes of 0.44 nm and 0.25 nm can be indexed to the (103) plane of SiC and (311) plane of $MnCo_2O_4$ [3,6,17]. The EDS maps of C, Co, Mn, Si, and O in Fig. 2(j) confirm the preparation of orderly $MnCo_2O_4$/SiC composite, consistent with the EDS spectrum of $MnCo_2O_4$/SiC (Fig. 2d). Fig. 3a shows the X-ray diffraction (XRD) patterns of $MnCo_2O_4$/SiC. The broad diffraction peaks at 30.5°, 35.9°, 37.6°, 43.7°, 54.3°, 57.9°, and 63.6° are related to the (220), (311), (222), (400), (422), (511), and (440) planes of the spinel type $MnCo_2O_4$ (JCPDS 23–1237) (marked with a solid circle) [12]. Three characteristic (1 1 1), (220), and (311) diffraction peaks at 2θ = 35.5°, 60.1°, and 75.2° are identified (SiC: JCPDS 29–1131) (marked with diamond) verifying the successful synthesis of the composite.

The CV curves of three electrodes are indicated in Fig. 3b-d, indicating the $MnCo_2O_4$/SiC/Ni-foam electrode have the superior electrochemical performance. Fig. 3e shows the CV curves of $MnCo_2O_4$/SiC||AC at different scanning rates between 10 and 160 mV s^{-1}. With increasing scanning rates, the area under the CV curve increases, but the shape of the CV curves with the redox current peaks does not change, indicating excellent reversibility and rates. Fig. 3f shows the GCD curves of $MnCo_2O_4$/SiC||AC in the voltage range between 0 and 1.5 V at different current densities, the supercapacitor achieve superior coulombic efficiency around 100 %. The specific capacitances are calculated to be 1.73, 1.08, 0.90, 0.81, and 0.70F cm^{-2} at current densities of 10, 15, 20, 25, and 30 mA cm^{-2} between 0 and 1.5 V (Fig. 3g). Discharging plateaus are not observed from the GCD curves, revealing strong Faradic reactions and good correlation with CV. The device shows outstanding long-term cycle stability with negligible capacitance decrease after 10,000 cycles (92.1 % capacitance retention), as shown in Fig. 3h. The device has a promising energy density of 90.3 Wh kg^{-1} at a large power density of 1.25 kW Kg^{-1}. Fig. 3i. shows ASC electrode has a series resistance R_s of 1.0 Ω (charge transfer resistance R_{ct} = 1.8 Ω) before cycling, which is smaller than 1.9 Ω of the ASC (R_{ct} = 17.8 Ω) after cycling, implying shorter ion diffusion and better electric conductivity.

The urchin-like and hexagonal $MnCo_2O_4$/SiC composite with a large specific surface area and abundant exposure of electro-active materials to the electrolyte has a high rate and energy density. For comparison, the properties and stability of $MnCo_2O_4$/SiC are better than those of recently reported $MnCo_2O_4$-based electrodes such as $MnCo_2O_4/Co_3V_2O_8$ [12], $MnCo_2O_4$@$Co(OH)_2$ [13], $MnCo_2O_4$/NiCo-LDH [14], $MnO_2/MnCo_2O_4$

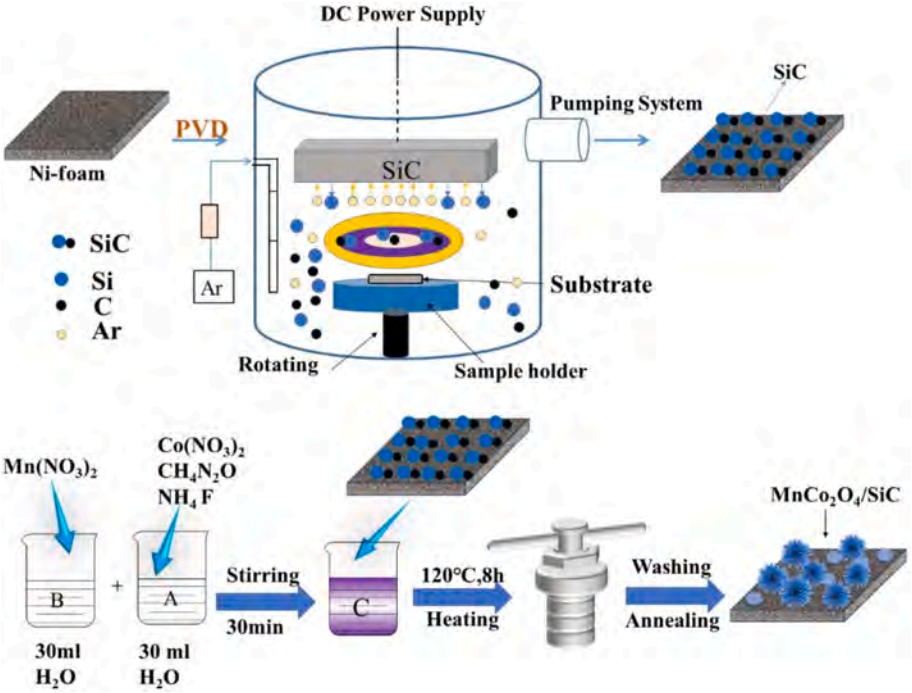

Fig. 1. Schematic illustration of the synthesis of the urchin-like and hexagonal $MnCo_2O_4$/SiC composite on Ni foam.

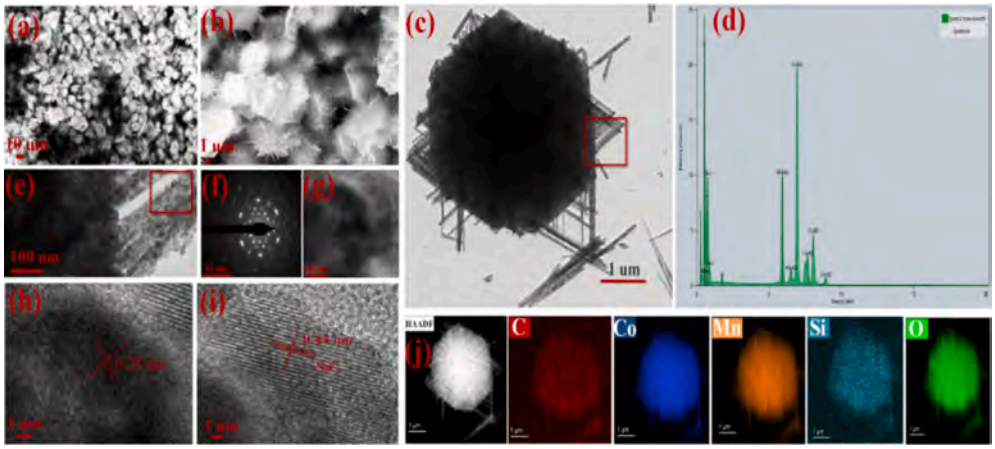

Fig. 2. (a-b) SEM images, (c) TEM image, (d) EDS spectrum, (e-i) HR-TEM spectra, and (j) EDS elemental maps of the urchin-like and hexagonal $MnCo_2O_4$/SiC composite on Ni foam.

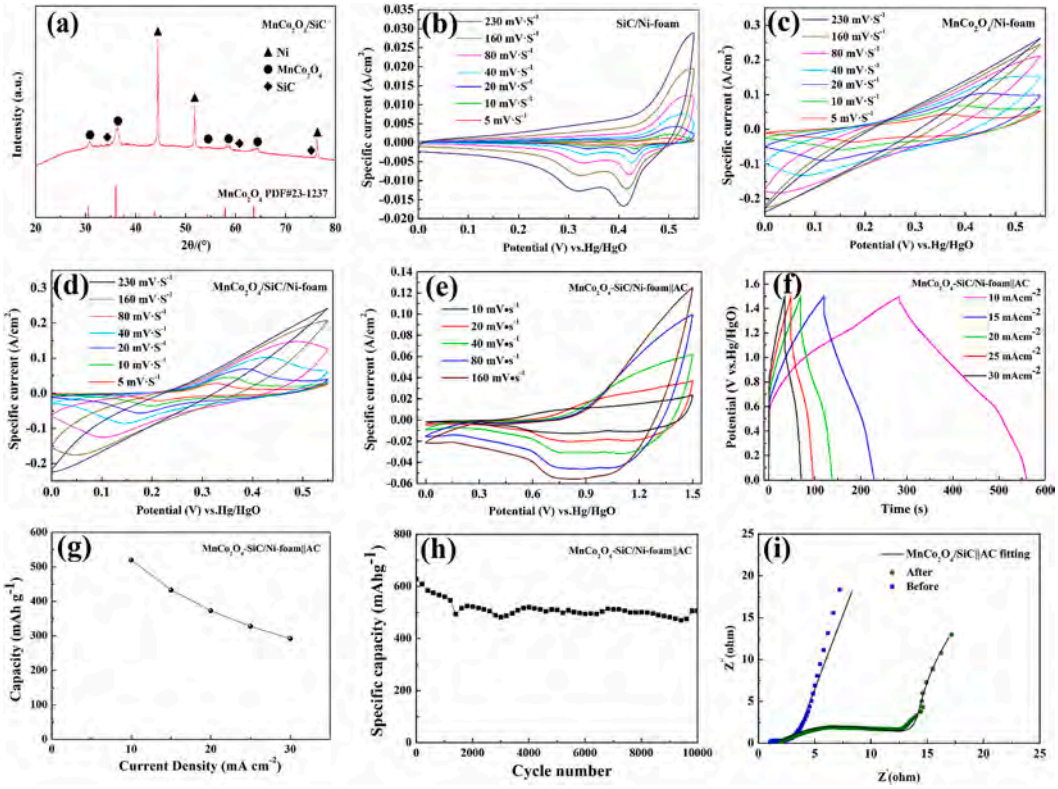

Fig. 3. (a) XRD patterns of $MnCo_2O_4$/SiC, (b-d) CV curves of SiC/Ni-foam, $MnCo_2O_4$/Ni-foam and $MnCo_2O_4$/SiC/Ni-foam, (e-f) CV and GCD curves of $MnCo_2O_4$/SiC||AC, (g) Specific capacitances of the $MnCo_2O_4$/SiC||AC, (h) Cycling stability of the $MnCo_2O_4$/SiC||AC at a current density of 10 mA cm^{-2}, and (i) Nyquist plots of the $MnCo_2O_4$/SiC||AC.

[10], and $MnCo_2O_4$ nanowires [4], as shown in Table 1. All in all, the composite has excellent properties and stability in supercapacitors.

4. Conclusion

The urchin-like and hexagonal $MnCo_2O_4$/SiC composite with excellent electrochemical properties is designed and fabricated. The $MnCo_2O_4$/SiC||AC ASC has an energy density of 90.3 Wh/kg (1.73F cm^{-2}) at the power density of 1.25 kW/kg, which is superior to that of similar materials reported in the literature. The strategy and materials described here have large potential in high-energy–density storage devices.

CRediT authorship contribution statement

Dajun Wu: Writing – review & editing, Writing – original draft, Project administration. **Panyi Wu:** Writing – original draft, Formal analysis, Data curation. **Zhengpeng Xia:** Software, Formal analysis, Conceptualization. **Xuekun Hong:** Supervision, Project administration. **Bin Qian:** Visualization, Methodology, Funding acquisition. **Paul K. Chu:** Writing – review & editing, Visualization, Data curation.

Declaration of competing interest

The authors declare that they have no known competing financial

Table 1
Specific capacitances of recently reported $MnCo_2O_4$-based electrodes.

Materials	Energy Densities (Wh kg^{-1})	Power Densities (kW kg^{-1})	Electrolytes	References
$MnCo_2O_4$/$Co_3V_2O_8$	37.5	0.75	3 M KOH	[12]
$MnCo_2O_4$@Co(OH)$_2$	55.42	0.80	3 M KOH	[13]
$MnCo_2O_4$/NiCo-LDH	21.3	0.16	PVA/KOH	[14]
MnO_2/$MnCo_2O_4$	40.8	0.26	3 M KOH	[10]
$MnCo_2O_4$ nanowires	25.4	0.78	2 M KOH	[4]
$MnCo_2O_4$/SiC	90.3	1.25	2 M KOH	This work

interests or personal relationships that could have appeared to influence the work reported in this paper.

Acknowledgments

This work was jointly supported by the National Natural Science Foundation of China (Grant No.11705015, No.62274017), National Science Foundation of Jiangsu Educational Department (Grant No. 15KJA430001), and City University of Hong Kong Donation Research Grants (Grant Nos. 9220061 and DON-RMG 9229021).

Data availability

Data will be made available on request.

References

[1] K.N. Hui, K.S. Hui, Z. Tang, V.V. Jadhav, Q.X. Xia, J. Power Sources 330 (2016) 195–203.
[2] C.V.V. Muralee Gopi, R. Ramesh, H.-J. Kim, J. Energy Storage 47 (2022) 103603.
[3] P.S. Pawar, P.A. Shinde, A.P. Torane, J. Mater Sci-Mater El. 34 (2023) 1020.
[4] X. Du, J. Sun, R. Wu, E. Bao, C. Xu, H. Chen, Nanoscale Adv. 3 (2021) 4447–4458.
[5] S.G. Krishnan, M. Harilal, N. Arshid, P. Jagadish, M. Khalid, L.P. Li, J. Energy Storage 44 (2021) 103556.
[6] Z. Zhu, Z. Zhang, Q. Zhuang, F. Gao, Q. Liu, X. Zhu, M. Fu, J. Power Sources 492 (2021) 229669.
[7] R.S. Redekar, A.T. Avatare, J.L. Chouhan, K.V. Patil, O.Y. Pawar, S.L. Patil, A. A. Bhoite, V.L. Patil, P.S. Patil, N.L. Tarwal, Chem. Eng. J. 450 (2022) 137425.
[8] L. Song, X. Zhang, S. Zhu, Y. Xu, Y. Wang, Sci. China Mater. 65 (10) (2022) 2871–2878.
[9] I.A. Alsafari, Opt. Mater. 138 (2023) 113592.
[10] Y. He, X. Pan, L. Kuang, B. Hu, Q. Zha, X. Chen, J. Nanopart. Res. 23 (2021) 54.
[11] X. Chen, W. Wang, X. Pan, C. Qiu, J. Energy Storage 43 (2021) 103238.
[12] R. Yu, Z. Li, Q. Wang, J. Solid. State. Chem. 329 (2024) 124440.
[13] M. Xiao, X. Niu, S. Yang, W. Zhang, T. Zhao, J. Solid. State. Chem. 26 (2022) 1703–1714.
[14] Y. Wang, Z. Wang, X. Zheng, X. Teng, L. Xu, Y. Yuan, X. Liu, A. Fu, Y. Li, H. Li, J. Alloy. Compd. 904 (2022) 164047.
[15] S. Kumar, G. Saeed, L. Zhu, K.N. Hui, N.H. Kim, J.H. Lee, Chem. Eng. J. 403 (2021) 126352.
[16] C.H. Chang, B. Hsia, J.P. Alper, S. Wang, L.E. Luna, C. Carraro, S.Y. Lu, R. Maboudian, Acs Appl. Mater. Interfaces 7 (48) (2015) 26658–26665.
[17] A. Sanger, A. Kumar, P.K. Jain, Y.K. Mishra, R. Chandra, Ind. Eng. Chem. Res. 55 (35) (2016) 9452–9458.
[18] M. Kim, J. Yoo, J. Kim, Chem. Eng. J. 324 (2017) 93–103.